Effects of Olefin-Based Compatibilizers on the Morphology, Thermal and Mechanical Properties of ABS/Polyamide-6 Blends

Guralp Ozkoc,[1] Goknur Bayram,[2] Erdal Bayramli[3]

[1]*Department of Polymer Science and Technology, Middle East Technical University, 06531 Ankara, Turkey*
[2]*Department of Chemical Engineering, Middle East Technical University, 06531 Ankara, Turkey*
[3]*Department of Chemistry, Middle East Technical University, 06531 Ankara, Turkey*

Received 7 June 2006; accepted 4 November 2006
DOI 10.1002/app.25848
Published online in Wiley InterScience (www.interscience.wiley.com).

ABSTRACT: In this study, commercially available epoxidized and maleated olefinic copolymers, EMA-GMA (ethylene-methyl acrylate-glycidyl methacrylate) and EnBACO-MAH (ethylene-*n* butyl acrylate-carbon monoxide-maleic anhydride), were used at 0, 5, and 10% by weight to compatibilize the blend composed of ABS (acrylonitrile-butadiene-styrene) terpolymer and PA6 (polyamide 6). Compatibilizing performance of these two olefinic polymers was investigated from blend morphologies, thermal and mechanical properties as a function of blend composition, and compatibilizer loading level. Scanning electron microscopy (SEM) studies showed that incorporation of compatibilizer resulted in a fine morphology with reduced dispersed particle diameter at the presence of 5% compatibilizer. The crystallization behavior of PA6 phase in the blends was explored for selected blend compositions by differential scanning calorimetry (DSC). At high compatibilizer level a decrease in the degree of crystallization was observed. In 10% compatibilizer containing blends, formation of γ-crystals was observed contrary to other compatibilizer compositions. The behavior of the compatibilized blend system in tensile testing showed the negative effect of using excess compatibilizer. Different trends in yield strengths and strain at break values were observed depending on compatibilizer type, loading level, and blend composition. With 5% EnBACO-MAH, the blend toughness was observed to be the highest at room temperature. © 2007 Wiley Periodicals, Inc. J Appl Polym Sci 104: 926–935, 2007

Key words: ABS; polyamide 6; compatibilization; polymer blend

INTRODUCTION

Polyamide 6 (PA6) is a widely used engineering polymer having good mechanical strength, chemical resistance, and high heat distortion temperature. However, PA6 has some disadvantages, such as notch-sensitivity under impact loading and relatively high moisture absorption; therefore, it is blended with other polymers to overcome these disadvantages. Because of the highly polar structure of polyamides, they form mostly immiscible blends with nonpolar polymers during blending. Compatibilization of polyamide blends using reactive constituents to form *in situ* block or graft copolymer at the interface is the frequently used method to achieve stable blend morphology and improved properties.

Blends of PA6 with acrylonitrile-butadiene-styrene terpolymer (ABS) are commercially important because of its improved toughness, dimensional stability, good surface texture, and processability. There is a great interest to compatibilize PA6/ABS blends using compatibilizers, which are capable of reacting with amine and/or acid end groups of PA6 and miscible with styrene-acrylonitrile (SAN) copolymer phase of ABS.[1–9]

Kim and Lee used styrene-maleic anhydride copolymer (SMA) to compatibilize the PA6/ABS blends, to observe the effects of blending sequence on the thermal and rheological properties and morphologies.[10] They concluded that SMA was an effective compatibilizer for a definite blending sequence and increased thermal resistance and modulus of the blend. Majumdar et al. showed that there was an optimum level for SMA to achieve stable blend morphology.[2] In recent literature, it was reported that imidized acrylic copolymers (IA) yielded well-dispersed phase morphology together with small particle size and super toughness in PA6/ABS blends.[3–5] Moreover, maleated polymers such as maleated polyethylene-octene elastomers (POE-*g*-MA),[6] poly(*N*-phenylmaleimide styrene-maleic anhydride),[7] maleated polybutadiene (PB-*g*-MA),[8] poly(methyl methacrylate)-maleic anhydride copolymer (MMA-MA)[9] were commonly used as compatibilizers due to their reaction capability with polyamides in PA6/ABS system.

Correspondence to: G. Bayram (gbayram@metu.edu.tr).

Journal of Applied Polymer Science, Vol. 104, 926–935 (2007)

TABLE I
Specifications of the Materials Used in the Study

Material	Trade name and supplier	Specifications
ABS	Lustran ABS M203FC, Lanxess	Density: 1.05 g/cm^3 MFI (220°C and 10 kg): 32.5 g/10 min Standard impact strength, easy flowing
PA6	Teklamid 6, Polyone	Density: 1.13 g/cm^3 MFI (235°C and 2.16 kg): 34.25 g/10 min Natural, unfilled, extrusion grade
EMA-GMA	Lotader 8900, Arkema	MFI (190°C, 2.16 kg): 6 g/10min Melting point: 65°C Acrylic ester: 24 wt % GMA content: 8 wt %
EnBACO-MAH	Fusabond A MG423D, Dupont	MFI (190°C, 2.16 kg): 8 g/10 min Melting point: 62°C MAH content: 16.6 mg KOH/g[a]

[a] Determined in our laboratory according to the procedure elsewhere.[17]

In the current study, commercially available epoxidized and maleated olefinic copolymers, ethylene-methyl acrylate-glycidyl methacrylate (EMA-GMA), and ethylene-*n* butyl acrylate-carbon monoxide-maleic anhydride (EnBACO-MAH) were selected as the compatibilizers for ABS/PA6 blends. Epoxy and maleic anhydride groups are responsible for the *in situ* reaction with end-groups of PA6; MA and nBA are responsible for the miscibility with SAN[11–16] phase of ABS, and ethylene chains act as toughenners because of their relatively low glass transition temperatures. The effects of compatibilizer type and content on blend morphologies, mechanical, dynamic mechanical and thermal properties as the function of blend composition were investigated.

EXPERIMENTAL

Materials and processing

The materials used in this study are specified in Table I. Before blending, ABS and PA6 pellets were dried in vacuum at 80°C for 12 h, and EMA-GMA and EnBACO-MAH were dried at 50°C for 4 h. The ABS/PA6 ratio were 0/100, 20/80, 50/50, 80/20, and 100/0. The ABS/PA6 part was $(100 - x)$ % of the blend, where x is the compatibilizer weight percent in the blend, which varied as 0, 5, and 10. (ABS/PA6)/Compatibilizer batches at prearranged compositions were dry-mixed first, then processed in a corotating twin-screw extruder (Thermoprism TSE 16 TC, $L/D = 24$) at a screw speed of 200 rpm and a barrel temperature profile of 190-230-230-235-240°C. The extrudate was water cooled and chopped into small pellets. The produced pellets were again vacuum-dried at 80°C for 12 h before injection molding. The specimens for mechanical and dynamic mechanical tests were molded by using a laboratory scale injection-molding machine (Microinjector, Daca Instruments) at a barrel temperature of 230°C and mold temperature of 80°C.

Scanning electron microscopy and image analysis

The cryogenically fractured sample surfaces were analyzed by using a low voltage SEM (JEOL JSM-6400) to observe the morphologies of the blends. PA6 and ABS phases were etched by immersing the fracture surfaces in formic acid for 15 min and in THF for 60 min, respectively. To prevent arcing sample surfaces were coated with gold. To calculate the apparent dispersed particle diameter, the area of the particles was measured automatically using an image analyze software (Image J 1.36, USA), then apparent diameters, d_{app}, were calculated using Eq. (1) by assuming globular particles:

$$d_{app} = 2(A/\pi)^{1/2} \tag{1}$$

where A is the area of the particle analyzed, which was obtained as an output using software. The distribution of d_{app} was obtained by measuring at least 300 particles. The average apparent diameters, $(d_{app})_{avg}$, were calculated using Eq. (2):

$$(d_{app})_{avg} = \left(\sum n_i d_i\right) \Big/ \left(\sum n_i\right) \tag{2}$$

where n is the number of the particle with apparent diameter size, d.

Differential scanning calorimeter

Differential scanning calorimeter (DSC) analyses were carried out by using a PerkinElmer Diamond DSC at a scanning rate of 10°C/min between 25 and 250°C temperature under N_2 atmosphere. The samples were first heated to 250°C and kept at this tem-

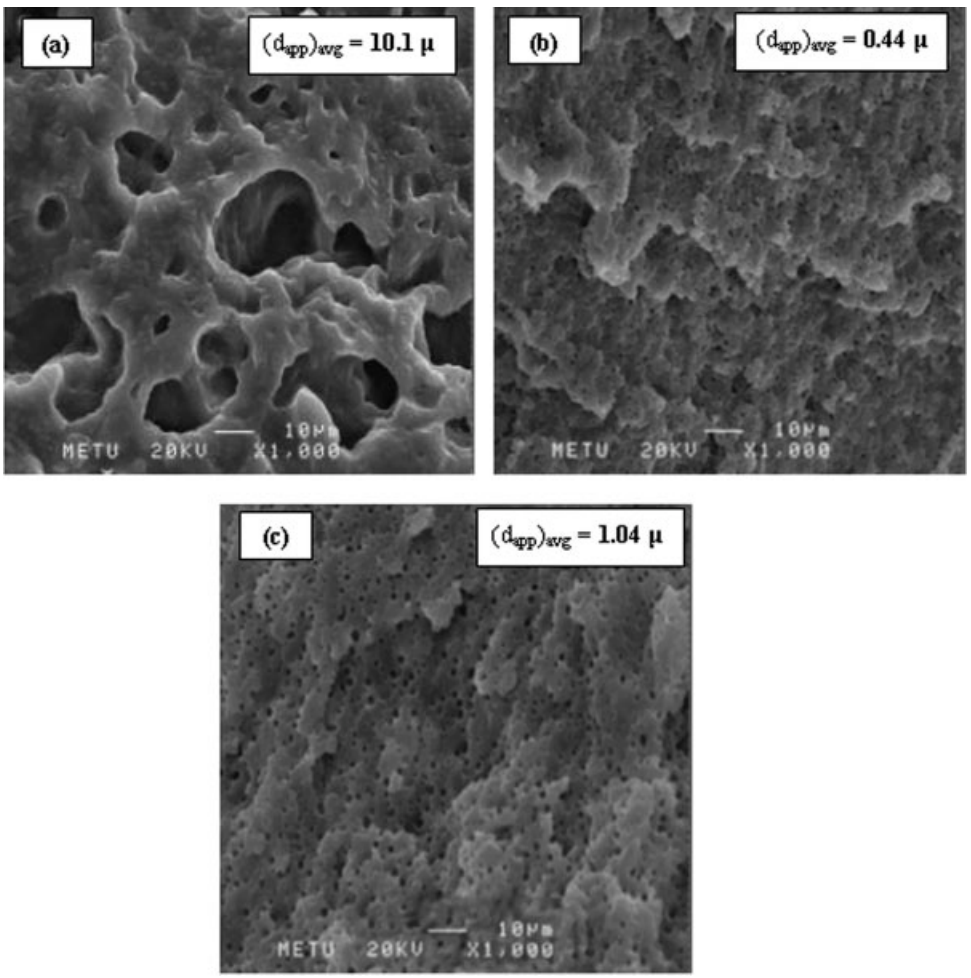

Figure 1 Scanning electron micrographs (×1000) of compatibilized and incompatibilized blends containing (20%PA6 + 80%ABS) + 5% compatibilizer. (a) No compatibilizer; (b) EnBACO-MAH; (c) EMA-GMA (PA6 phase was etched with formic acid).

perature for 3 min to erase any thermal history, then cooled to room temperature. They were again heated to 250°C as the second heating run.

Dynamic mechanical analysis

Dynamic mechanical analysis (DMA) tests were performed on rectangular samples with the dimensions of 6 × 60 × 2 mm^3 using PerkinElmer Pyris Diamond DMA instrument operating in bending mode. Measurements were taken at a frequency of 1 Hz. Temperature was raised from −150 to 150°C at a scanning rate of 5°C/min.

Mechanical properties

Tensile tests were carried out at room temperature according to ASTM D 658 using Lloyd 30 K universal testing machine. The crosshead speed was 5 mm/min. At least five samples were tested and average results with standard deviations were reported for each type of blend. Charpy impact tests were performed by using a pendulum impact tester of Coesfeld Material Test, according to the ASTM D 256 at room temperature. The notches were machined according to the relevant standard.

RESULTS AND DISCUSSION

Scanning electron microscopy and image analysis

The morphologies of (ABS/PA6)/5% compatibilizer blend system were examined in terms of blend ratio and compatibilizer type. The scanning electron micrographs of (80/20)/5% compatibilizer blend system as a function of compatibilizer type can be observed in Figure 1(a–c), and corresponding distributions of dispersed phase apparent diameters are shown in Figure 2. The continuous phase is ABS and the dispersed phase is PA6. The black holes seen in the micrographs were the vacancies left after the removal of PA6 by formic acid extraction. The irregu-

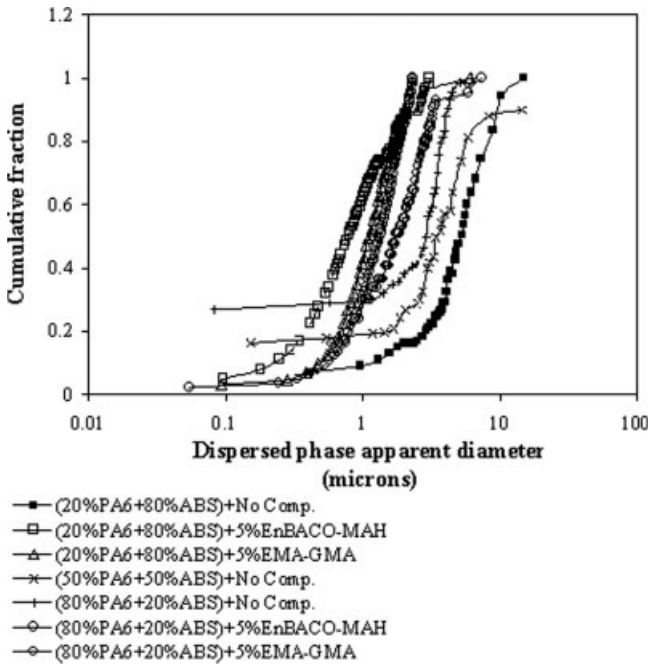

Figure 2 Dispersed phase apparent diameter distribution for the compatibilized and incompatibilized ABS/PA6 blend system.

lar, coarse ($(d_{app})_{avg}$ = 10.1 μm), nonelliptical dispersed morphology of PA6 in ABS matrix in the absence of compatibilizers became a fine ($(d_{app})_{avg}$ = 0.44 μm for EnBACO-MAH and $(d_{app})_{avg}$ = 1.04 μm) for EMA-GMA), elliptical morphology with the addition of compatibilizers [Fig. 1(a–c)]. Incorporation of the compatibilizer reduces the interfacial tension between ABS/PA6 phases that results in a fine dispersion of PA6 in melt state during preparation of blends.[18] Moreover, the addition of compatibilizers reduces the droplet coalescence rates because of steric repulsion[19–21]; therefore, finely dispersed phase morphology with relatively small particles can be obtained in the presence of effective compatibilizers. In the current system, possible chemical reactions lead to the finely dispersed morphology due to the reactions between maleic anhydride with amine end-group and epoxy groups with amide and/or acid end-groups of PA6 for EnBACO-MAH and EMA-GMA, respectively. These reactions are shown in Figures 3 and 4. The scanning electron micrographs show that EnBACO-MAH has a higher compatibilization capability than EMA-GMA for ABS/PA6 system taking into account the sizes of the dispersed PA6 domains concerned.

The scanning electron micrographs of (50/50)/5% compatibilizer system with the two compatibilizers are shown in Figure 5(a–c). The holes in the pictures are the vacancies left after the removal of PA6 by formic acid extraction. In the case of no compatibilizer, the discontinuous phase is PA6. This dispersed morphology became cocontinuous when compatibilizers were added. The possible reason can be the increased viscosity of PA6 as a result of grafting reactions with the compatibilizers; hence, the viscosity ratio of ABS to PA6 becomes close to the volumetric ratio, which is the criterion to obtain cocontinuity according to Paul Barlow model.[24] The size of the undulations seen on the surface is different for each compatibilizer type. In the case of EnBACO-MAH, the sizes of the undulations are smaller than those of EMA-GMA.

For (20/80)/5% compatibilizer system, the dispersed ABS domains in the PA6 matrix are seen as black holes left after the removal of ABS by THF extraction [Fig. 6(a–c)]. The addition of compatibilizers decreased the diameter of ABS domains ($(d_{app})_{avg}$ = 9.97 μm) for no compatibilizer, $(d_{app})_{avg}$ = 0.86 μm for EnBACO-MAH, and $(d_{app})_{avg}$ = 1.20 μm for EMA-GMA) significantly. The average diam-

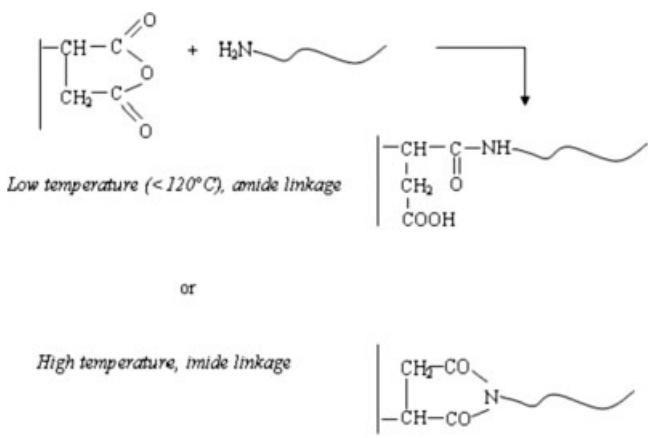

Figure 3 Reaction scheme of maleic anhydride group with amide end groups of PA6.[22]

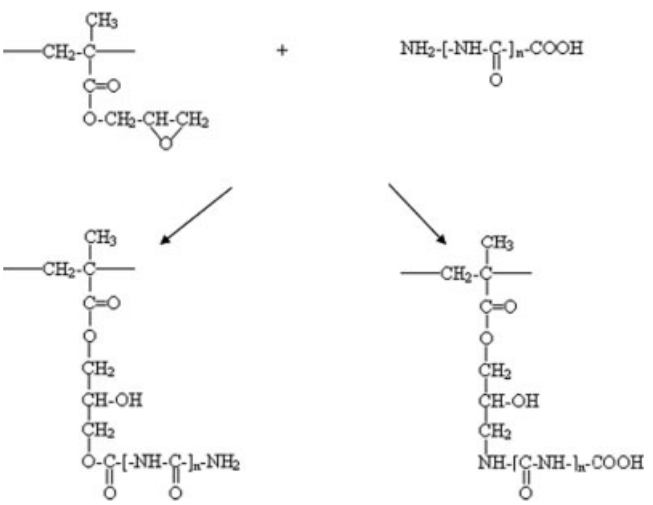

Figure 4 Reaction scheme of epoxide group with acid and amide end groups of PA6.[23]

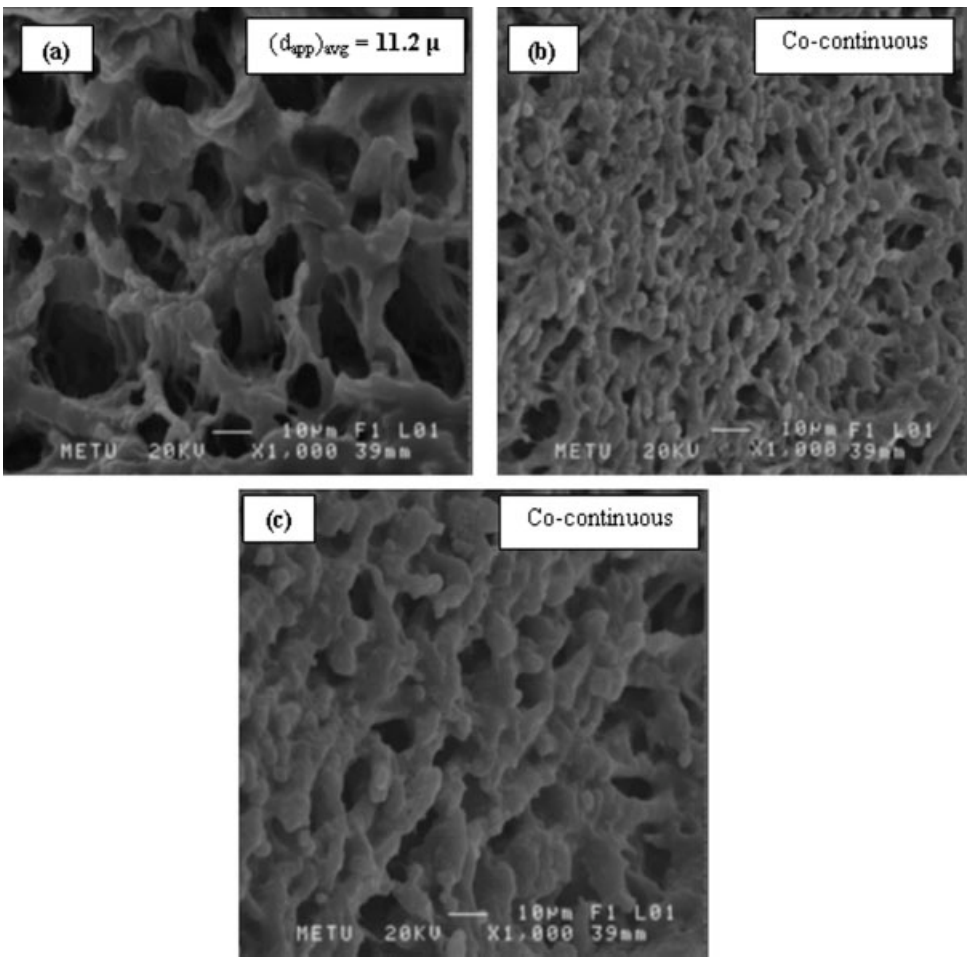

Figure 5 Scanning electron micrographs (×1000) of compatibilized and incompatibilized blends containing (50%PA6 + 50%ABS) + 5% compatibilizer. (a) No compatibilizer; (b) EnBACO-MAH; (c) EMA-GMA (PA6 phase was etched with formic acid).

eter of the ABS domains in the case of EnBACO-MAH is smaller than that of EMA-GMA.

When the compatibilization efficiency of these two olefin-based copolymers were compared, EnBACO-MAH seemed to be more effective than EMA-GMA copolymer due to the smaller dispersed particle apparent diameters of the blend for (80/20) and (20/80) at 5% compatibilizer content. It has been proposed that the final morphology is highly dependent on the topology of grafting.[25–27] In the case of blends prepared using EMA-GMA, which is difunctional with respect to PA6 (i.e., possible reactions with both amine and acid ends), dense locals of PA6-*graft*-EMA-GMA with high probability of two point grafting that results in cross-links can form in the early stages of extrusion, which can hinder further particle breakdown in the downstream of extruder.[14,28]

It should also be noted that breakup of the dispersed phase is another process that takes place during melt-compounding, which determines the final morphology together with interfacial interactions.[28] It highly depends on the viscosity ratio of components. However, in the current article, the rheological properties of the materials produced were not measured.

Differential scanning calorimeter analysis

DSC was used to examine the melting and crystallization behavior of the PA6 component in the blends. Melting point (T_m, °C), melting enthalpy (ΔH_f, J/g), and degree of crystallization (X_c, %) were obtained from second heating thermograms and crystallization temperature (T_c) were obtained from cooling thermograms for PA6 phase in the blends. ΔH_f in the second heating thermogram was used for calculation of degree of crystallinity of the PA6 part of the blends using following equation:

$$X_c(\%) = \frac{\Delta \mathrm{H_f}}{(\mathrm{F})(\Delta \mathrm{H_f^*})} \times 100 \qquad (3)$$

where F is the weight fraction of PA6 in the blend and ΔH_f^* is the extrapolated value of the enthalpy corresponding to the melting of 100% crystalline pure PA6.

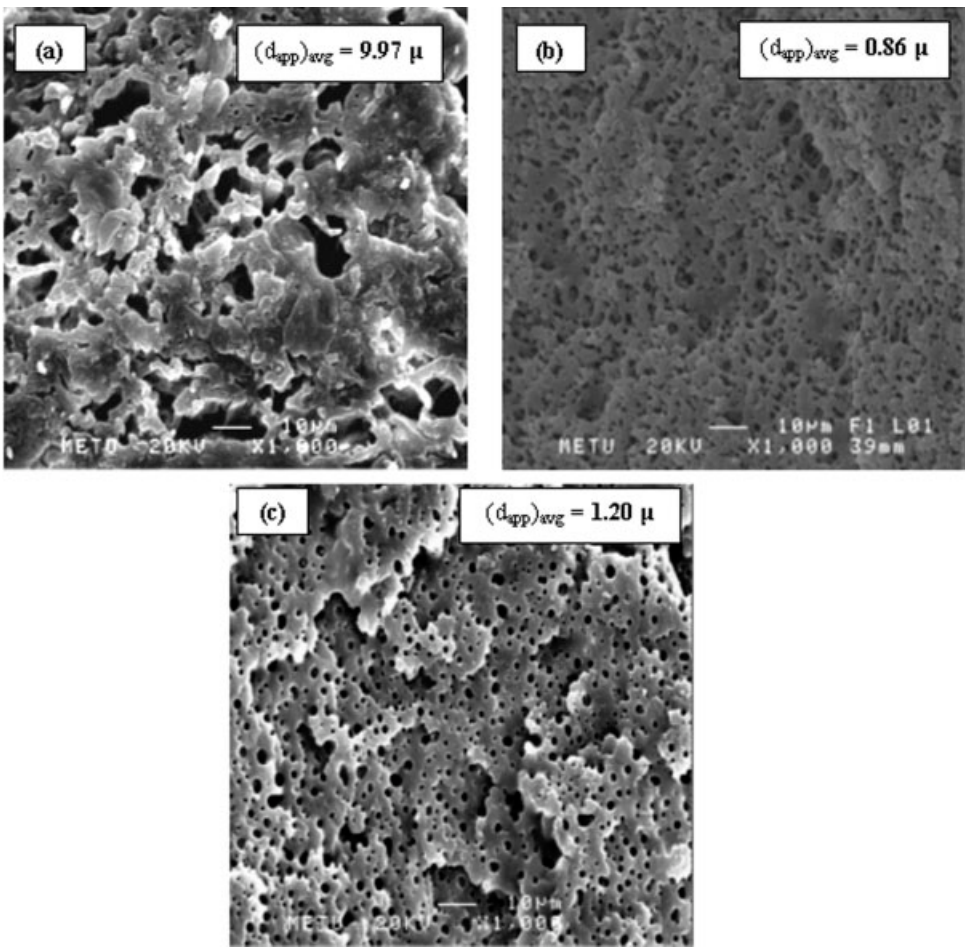

Figure 6 Scanning electron micrographs (×1000) of compatibilized and incompatibilized blends containing (80%PA6 + 20%ABS) + 5% compatibilizer. (a) No compatibilizer; (b) EnBACO-MAH; (c) EMA-GMA (ABS phase was etched with THF).

Table II shows that the addition of ABS to the pure PA6 did not affect the melting temperature of the system in the absence of a compatibilizer. However, compatibilized blends exhibited a lower melting temperature with respect to both pure PA6 and incompatibilized 50/50 blend system. Depression in T_m about 2–5°C can be considered as the interfacial compatibility of the system is improved with the addition of the compatibilizer.[30–33] Probably, the addition of compatibilizers to the ABS/PA6 blends has a negative effect on crystallization of PA6 due to the interfacial interaction and formation of PA6-*graft*-compatibilizer molecules that are less perfect than pure PA6.

(50/50)/10%EnBACO-MAH and (50/50)/10%EMA-GMA blends exhibited two melting peaks in the second heating thermograms given in Figure 7. This result

TABLE II
Results of DSC Analysis

No.	(ABS/PA6)/Comp.	T_m (°C)	ΔH_f (J/g)	X_c (%)	T_c (°C)
1	PA6	224.9	65.8	28.6	191.2
2	(50/50)/No Comp.	224.3	23.4	20.4	187.2
3	(50/50)/5 EMA-GMA	222.6	22.8	20.9	184.6
4	(50/50)/10 EMA-GMA	213.9; 221.6	12.2	11.8	183.5
5	(50/50)/5 EnBACO-MAH	221.5	22.0	20.1	183.8
6	(50/50)/10 EnBACO-MAH	214.5; 220.3	13.2	12.7	182.2
7	(80/20)/5 EnBACO-MAH	221.3	10.0	22.9	181.8
8	(20/80)/5 EnBACO-MAH	222.4	36.5	20.8	183.5
9	(80/20)/5 EMA-GMA	222.4	9.9	22.8	183.2
10	(20/80)/5 EMA-GMA	222.2	38.4	22.0	183.2

Specific heat of fusion for 100% crystalline PA6 (ΔH_f^*) is 230 J/g.[29]

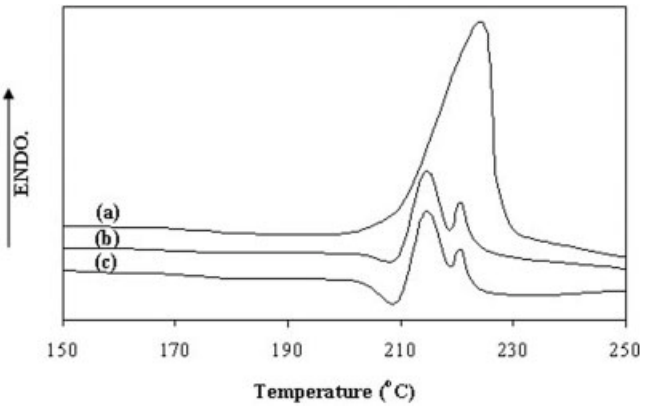

Figure 7 Representative thermograms for the melting behavior of ABS/PA6 blends: (a) 50/50, (b) (50/50)/10 EnBACO-MAH, (c) (50/50)/10 EMA-GMA.

shows that there are two different structures of crystals formed during cooling. At first around 214°C, the major peak shows that the less perfect γ-crystals formed in the cooling step melt. Around 221°C (the minor peak), the more stable α-crystals melt.[34] The small exotherm observed before the major melting peak is the reorganization of the less perfect PA6 crystals. These crystals are the monoclinic γ-crystals of the PA6.[34,35] The formation of this structure in the presence of 10% compatibilizer may be as a consequence of increased extent of reaction between PA6 and maleic anhydride; so the formation of thermally stable α-crystals is hindered because of this grafting reaction.[36,37] This phenomenon is also observed from the X_c and T_c, which are lower when compared to other blend systems. The chemical reaction leading to increase in the viscosity of the media can decrease the crystallization rate and crystal growth.[37]

The degree of crystallinity of the blends is lower than that of PA6. The presence of the second phase inhibits the crystallization and the crystallization ability of PA6 was detrimentally influenced. This effect can also be observed from T_c values. Addition of the second phase together with a compatibilizer further decreases the crystallization temperature as a result of retardation effect of increased viscosity due to the compatibilization reactions.

Dynamic mechanical analysis

DMA is used to study the miscibility of the ABS and PA6 in the presence of the olefin-based copolymers. Figure 8 shows the DMA curves of the some selected blend systems. The peaks at −69.2°C and 110.3°C are the T_g's of the polybutadiene (PB) and poly (styrene-*co*-acrylonitrile) (SAN) phase of ABS, respectively. The T_g peak of PA6 is seen at 34.8°C. When the incompatibilized 50/50 blend system is considered, it is observed that the T_g's of the PB and SAN phase of ABS and PA6 are not shifted. If the phases were immiscible, they would have exhibited their own T_g after blending.[29] When the compatibilizers were incorporated to the system, the T_g of both SAN and PA6 phases were shifted to the lower values probably due to the lower T_g values of the PA6-*g*-compatibilizer molecules. This shows the partial miscibility of phases within each other by the addition of the compatibilizer. With the addition of the compatibilizers, the damping peaks are broadened, and this can be ascribed to the increased length of the interfacial region, probably due to the formation of PA6-*g*-compatibilizer at the interphase.[38] There is no significant effect of the compatibilizer type, compatibilizer content, and blend composition in DMA curves.

Mechanical properties

Figure 9 shows the variation of yield strength with respect to PA6 and compatibilizer content. In the absence of compatibilizers, an increasing trend is observed after 50% PA6 content. The compatibilized blends containing 80% PA6 have higher strength values compared to other blends due to the continuous PA6 phase. The blends of 20 and 50% PA6 compatibilized with 5% olefinic polymer have improved yield strength values than those of incompatibilized ones owing to the improved adhesion at the interface because of the possible reactions given in Figures 3 and 4. However, the blends of 20 and 50% PA6 compatibilized with 10% olefinic polymer have lower yield strengths. Below the saturation level of compatibilizer, the bonded molecules are located in the interfacial area between the dispersed phase and

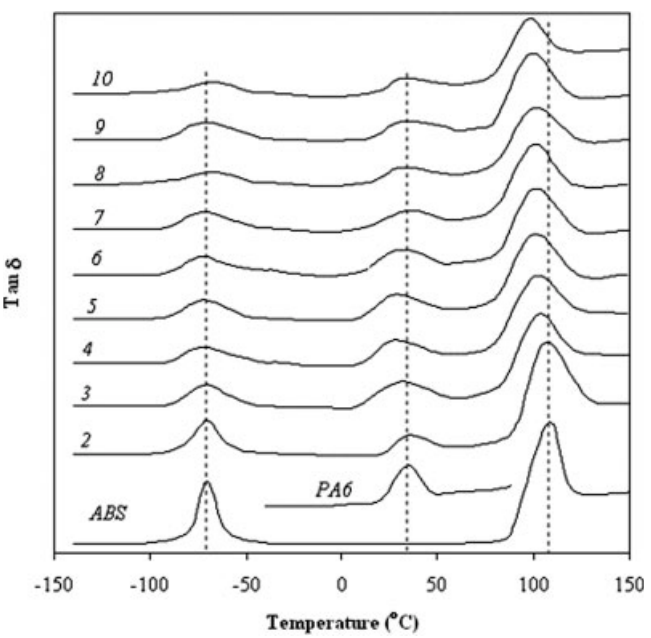

Figure 8 Representative tan δ curves for the blends obtained in DMA analysis (the numbers correspond to the blend system given in Table II).

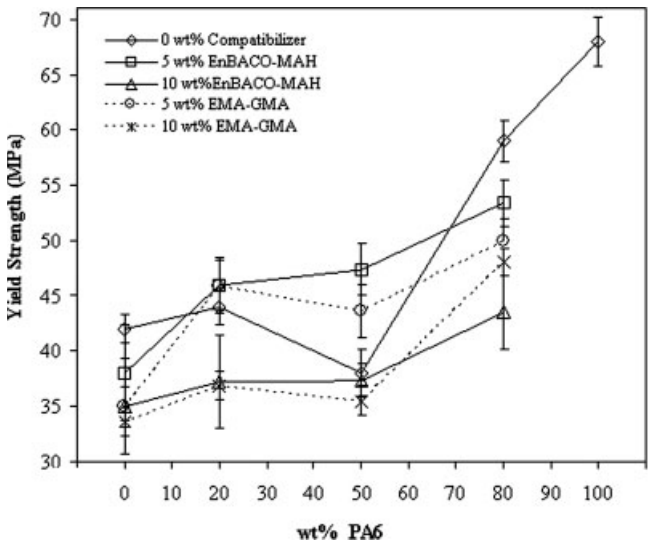

Figure 9 Variation of yield strength with respect to PA6 concentration and compatibilizer content.

matrix. When saturation level is exceeded, the compatibilizer forms a weak boundary layer between the ABS and PA6 phases resulting in low yield strength values. Thus, only required amount of compatibilizer should be used to improve the miscibility of the components.[39]

For the blends containing 80% PA6, the incompatibilized blends exhibit higher yield strengths. When all the yield strength data of tertiary blends are concerned, the strength values measured can not exceed that of neat-PA6 and all of them are greater than the yield strength of neat-ABS.

Variation of strain at break values with as a function of PA6 concentration and compatibilizer content can be seen in Figure 10. It is observed that the strain at break values of blends increase with the increasing amount of PA6 after 50% of PA6 because of the continuity of PA6 phase. Incompatibilized blends showed the lowest strain at break values when compared with the compatibilized ones and exhibits more brittle behavior during tensile testing. When the strain at break values of blends compatibilized with EMA-GMA are considered, as EMA-GMA concentration decreases strain at break values increases after 50% PA6 concentration. With both 5 and 10% EnBACO-MAH, the strain at break values are larger than 100% above 50% PA6 level.

The failure behavior of the blends showed differences. The photograph of some selected tensile specimens after testing is shown in Figure 11. It is observed that in the absence of olefin-based compatibilizers, blends with 20 and 50% PA6 failed in brittle manner without neck formation. Stress whitening, which is due to the light scattering from crazes in the matrix or cavities in the dispersed phase, can be observed. Even in the presence of compatibilizers, for the blends containing 20% PA6 exhibited brittle failure despite relatively higher elongation. The compatibilized blends containing 50% PA6 underwent necking and failed in ductile manner. When the continuous phase is PA6 (for blends containing 80%PA6), the specimens again deformed by neck formation, but this case after necking they underwent strain-hardening at the end of the tests, which resulted in an increase in measured ultimate stresses.

When the impact strength of blends are concerned, the incompatibilized blend exhibits decreasing trend in impact strength values, which can be observed in Figure 12, due to the coarse dispersed phase morphology seen in scanning electron micrographs. The

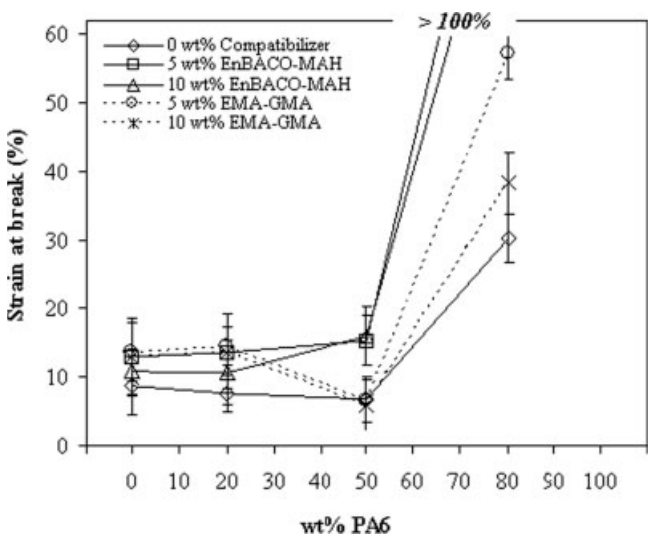

Figure 10 Variation of strain at break with respect to PA6 concentration and compatibilizer content.

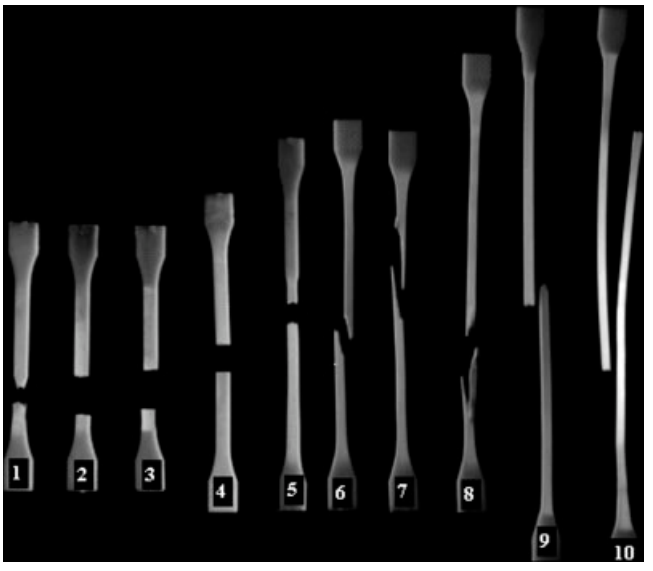

Figure 11 Selected tensile specimens after testing.

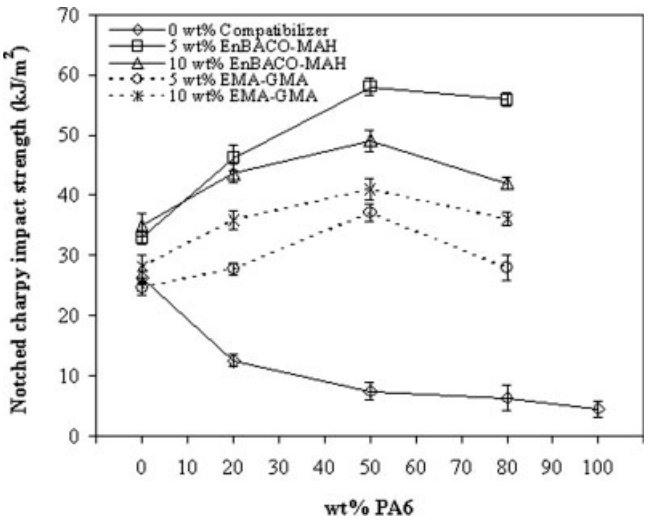

Figure 12 Variation of impact strength with respect to PA6 concentration and compatibilizer content.

incorporation of compatibilizers results in more than fourfold improvement. The impact strength of compatibilized blends increases as PA6 concentration increases up to 50% PA6. A maximum is obtained around 50% PA6 concentration regardless of the type and amount of compatibilizer possibility due to the cocontinuous morphology of the blend. Such kind of impact modification was reported in the literature for the cocontinuous polyoxymethylene/polyurethane blends. It was reported that an intermeshed network-like structure gave super tough material; whereas distributed rubber particles resulted in more than fourfold lower Izod impact strengths.[18,40]

The impact strength of the polymer blends is highly dependent on the size and dispersion of the second phase. There are two reasons why the dispersed particles in the matrix give higher toughness: to cavitate and hence change the stress state around the particles and to generate a local stress concentration.[41–43] However, the cavitated particle should not initiate the fracture process; therefore, these particles have to be very small and not grow to a size which can initiate a crack.[18] In literature, an optimum amount of compatibilizer, which can provide fine and well-dispersed blend morphology, was studied and the researchers found out that after saturation concentration of compatibilizer is exceeded, the impact properties either decreased or remained constant.[6,7,22,44]

In the current study, the compatibilizers used can act as toughening because of their elastomeric nature with low glass transition temperature. For a given PA6 content, the impact strength of the blends compatibilized with EnBACO-MAH gives higher toughness than EMA-GMA due to the finer morphologies obtained in the case of EnBACO-MAH at 5 and 10% loadings. For EnBACO-MAH, tougher blends are obtained at 5% loadings; however, for EMA-GMA, tougher blends are obtained at 10% loading level for a given PA6 concentration.

CONCLUSIONS

Blends of ABS and PA6 compatibilized with/without EnBACO-MAH and EMA-GMA at various amounts of range of blend composition were explored. Morphological studies indicated that incorporation of the maleated and epoxidized olefin based polymers compatibilize the ABS/PA6 polymers. When the compatibilization efficiencies were compared in terms of blend morphologies, it was observed that EnBACO-MAH resulted in finer dispersion of second phase than that of EMA-GMA. Compatibilized blends exhibited a lower melting temperature with respect to both pure PA6 and incompatibilized 50/50 blend system, which implies that the miscibility of the system was improved with the addition of the compatibilizers. When the compatibilizers were incorporated to the system, the T_g of both SAN and PA6 phases were shifted to the lower values observed from DMA. This was also a sign of the partial miscibility of phases within each others by the addition of the compatibilizer. Tensile behavior of the blends was complex, but in general, the yield strength of blends increased with the increasing amount of PA6 in the blend. The blends of 20 and 50% PA6 compatibilized with 5% olefinic polymer have improved yield strength. It was shown that excessive amounts of compatibilizer decreased the mechanical strength of the blends. Incompatibilized blends exhibited brittle fracture behavior in tensile testing; however, compatibilization increased the strain at break values of the blends. Incompatibilized blend showed decreasing trend in impact strength values. Incorporation of the compatibilizers improved the toughness of the blends significantly.

References

1. Majumdar, B.; Keskkula, H.; Paul, D. R. Polymer 1994, 35, 5468.
2. Majumdar, B.; Keskkula, H.; Paul, D. R. Polymer 1994, 5, 3164.
3. Kudva, R. A.; Keskkula, H.; Paul, D. R. Polymer 2000, 41, 225.
4. Kudva, R. A.; Keskkula, H.; Paul, D. R. Polymer 2000, 41, 239.
5. Kitayama, N.; Keskkula, H.; Paul, D. R. Polymer 2001, 42, 3751.
6. Chiu, H. T.; Hsiao, Y. K. Polym Eng Sci 2004, 44, 2340.
7. Lee, C. W.; Ryu, S. H.; Kim, H. S. J Appl Polym Sci 1997, 64, 1595.
8. Lai, S. M.; Liao, Y.-C.; Chen, T.-W. Polym Eng Sci 2005, 45, 1461.
9. Araujo, E. M.; Hage, E.; Carvalho, A. J. F. J Mat Sci 2004, 39, 1173.
10. Kim, B. K.; Lee, Y. M. Polymer 1993, 34, 2075.
11. Gan, P. P.; Paul, D. R.; Parwa, A. R. Polymer 1994, 35, 3513.

12. Nishimoto, M.; Keskkula, H.; Paul, D. R. Polymer 1989, 30, 1279.
13. Chu, J. P.; Paul, D. R. Polymer 1999, 40, 2687.
14. Kudva, R. A.; Keskkula, H.; Paul, D. R. Polymer 1998, 39, 2447.
15. Araujo, E. M.; Hage, E.; Carvalho, A. J. F. J Appl Polym Sci 2003, 37, 842.
16. Araujo, E. M.; Hage, E.; Carvalho, A. J. F. J Appl Polym Sci 2003, 90, 2643.
17. Sclavons, M.; Carlier, V.; De Roover, B.; Franquinet, P.; Devaux, J.; Legras, R. J Appl Polym Sci 1996, 62, 1205.
18. Paul, D. R.; Bucknall, C. B. Polymer Blends; Wiley: New York, 2000.
19. Creton, C.; Kramer, E. J.; Hui, C. Y.; Brown, H. R. Macromolecules 1999, 25, 3075.
20. Jin, K. K.; Hwayong, L. Polymer 1996, 37, 305.
21. Jeon, H. K.; Jin, K. K. Polymer 1998, 39, 6227.
22. Thomas, S.; Groeninckx, G. Polymer 1999, 40, 5799.
23. Tedesco, A.; Krey, P. F.; Barbosa, R. V.; Mauler, R. S. Polym Int 2001, 51, 105.
24. Paul, D. R.; Barlow, J. W. J Macromol Sci, Rev Macromol Chem 1980, 18, 109.
25. Majumdar, B.; Keskkula, H.; Paul, D. R. Polymer 1994, 35, 1386.
26. Majumdar, B.; Keskkula, H.; Paul, D. R. Polymer 1994, 35, 1399.
27. Oshinski, A. J.; Keskkula, H.; Paul, D. R. Polymer 1992, 33, 284.
28. Majumdar, B.; Paul, D. R.; Oshinski, A. J. Polymer 1997, 38, 1787.
29. Sudhin, D.; David, J. L. Polymer Compatibilizers; Hanser Publishers: Munich, 1996.
30. Hage, E.; Ferreira, L. A. S.; Manrich, S.; Pessan, L. A. J Appl Polym Sci 1999, 71, 423.
31. Gao, G.; Wang, J.; Jinghua, Y.; Yu, X.; Ma, R.; Tang, X.; Yin, Z.; Zhang, X. J Appl Polym Sci 1999, 72, 683.
32. Ju, M. Y.; Chang, F. C. Polymer 2000, 41, 1719.
33. Kim, B. O.; Woo, S. I. Polym Bull 1998, 41, 707.
34. Tol, R. T.; Mathot, V. B. F.; Reynaers, H.; Goderis, B.; Groeninckx, G. Polymer 2005, 46, 2966.
35. Ramesh, C.; Bhoje, G. E. Macromolecules 2001, 34, 3308.
36. Hou, L.; Yang, G. Macromol Chem Phys 2005, 206, 1887.
37. Sun, S. L.; Xu, X. Y.; Yang, H. D.; Zhang, H. X. Polymer 2005, 46, 7632.
38. Evstatiev, M.; Schultz, J. M.; Petrovich, S.; Georgiev, G.; Fakirov, S.; Friedrich, K. J Appl Polym Sci 1998, 67, 723.
39. Tang, T.; Huang, B. Polymer 1994, 35, 281.
40. Wadhwa, L. H.; Dolce, T. L.; La Nieve, H. L. SPE Rtec; Columbus: Ohio, 1985.
41. Bucknall, C. B. Toughened Plastics; Applied Science Publishers, Ltd: London, 1977.
42. Huang, J. J.; Paul, D. R. Polymer 2006, 41, 3505.
43. Dijkstra, K.; van der Wal, A.; Gaymans, R. J. J Mat Sci 1994, 29, 3489.
44. Liu, X.; La Mantia, F.; Scaffaro, R. J Appl Polym Sci 2002, 86, 449.